

# NIMFEIA

## Deliverable D3.4

### Report on the mode filtering technique implemented in micromagnetics code

---

Project Number	101070290
Project name	Nonlinear Magnons for Reservoir Computing in Reciprocal Space
Project acronym	NIMFEIA
Work Package	WP3 Modelling the magnon reservoir in the GHz regime
Type	Report
Dissemination level	Public
Lead Beneficiary	UPS
Due date of delivery	Month 4 – January 2023

## 1. Summary

This report describes the implementation of the mode filtering technique related to the initial Milestone 4 of Work Package 3 (*Modelling the magnon reservoir in the GHz regime*). The technique is used to estimate the population dynamics of a given eigenmode of the magnon reservoir directly from micromagnetics simulations. We present an application of this technique to a permalloy disk with a vortex ground state and show how transient three-magnon processes can be studied.

## 2. Background

Micromagnetic simulations perform a numerical time integration of the Landau-Lifshitz-Gilbert equation, which describes magnetization dynamics in the long-wavelength limit. The magnetic material studied is discretised using either the finite difference or finite element method, and the nonlinear partial differential equation

$$\frac{d\mathbf{m}_i}{dt} = -\gamma_0 \mathbf{m}_i \times \mathbf{H}_{\text{eff}} + \alpha \mathbf{m}_i \times \frac{d\mathbf{m}_i}{dt}, \quad (1)$$

which represents the time evolution of the normalized magnetization vector,  $\mathbf{m} = \mathbf{m}(\mathbf{r}, t)$ , is solved self-consistently for each finite difference or finite element cell  $i$ . Here,  $\gamma_0$  is the gyromagnetic constant,  $\mathbf{H}_{\text{eff}}$  is the effective field which encompasses all short- and long-ranged magnetic interactions present at site  $i$ , and  $\alpha$  is the Gilbert damping constant. More details on the method can be found in Ref. [1].

Here, we are interested in the nonlinear transient dynamics of particular spin wave eigenmodes of the system,  $\psi_k(\mathbf{r}, t)$ , rather than the magnetization  $\mathbf{m}(\mathbf{r}, t)$  itself. While  $\psi_k(\mathbf{r}, t)$  can, of course, be computed from  $\mathbf{m}(\mathbf{r}, t)$ , this is a computationally-intensive task at the post-processing step so it is more useful to develop a scheme in which  $\psi_k(\mathbf{r}, t)$  can be projected directly out from Eq. (1). To lowest order, the fluctuations in the magnetization can be expanded in terms of these eigenfunctions

$$\delta\mathbf{m}(\mathbf{r}, t) = \sum_k a_k(t) \psi_k(\mathbf{r}),$$

where  $a_k(t)$  are complex mode amplitudes, with the mode power being a measure of the mode population,  $n_k \propto a_k^* a_k = |a_k|^2$ . The goal is to obtain  $a_k(t)$  directly from the simulations for a given set of  $\psi_k(\mathbf{r})$  with a minimum of data post-processing.



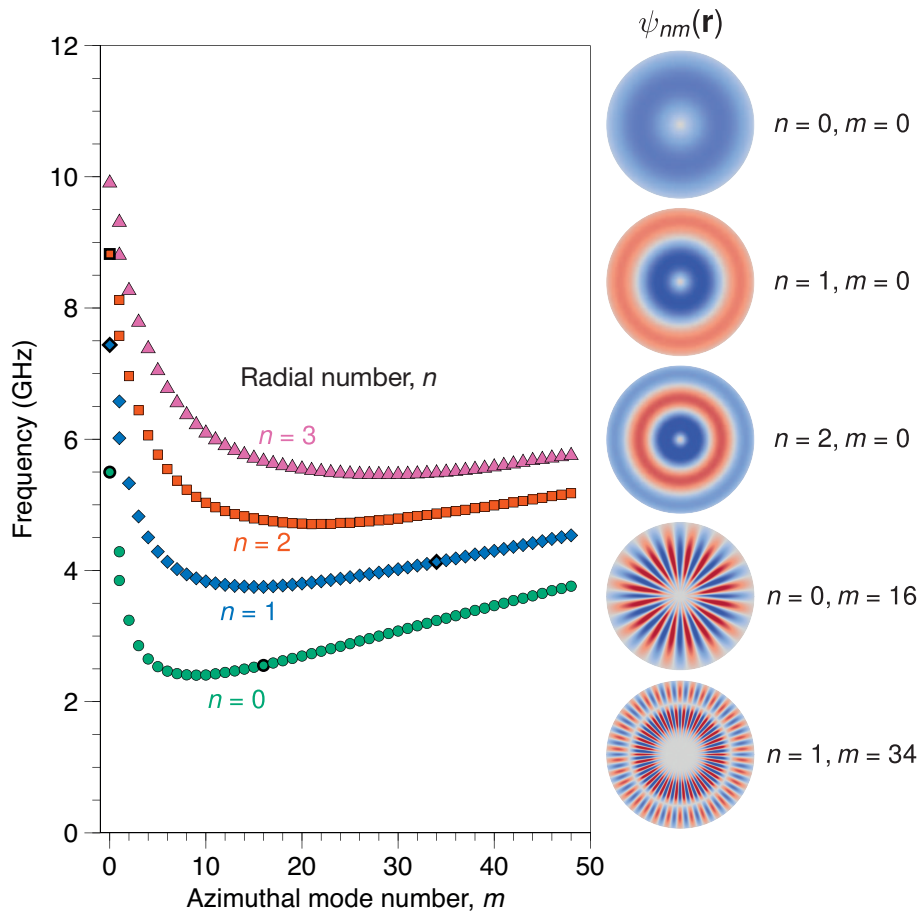


**Figure 1.** Dispersion relation of spin-wave eigenmodes in a 5- $\mu\text{m}$  diameter, 50-nm thick permalloy disk computed using MuMax3 micromagnetics simulations.  $n$  is the radial number and  $m$  is the azimuthal number. The right panel shows the spatial profiles of a few eigenmodes,  $\psi_{nm}(\mathbf{r})$ , whose frequencies are indicated by symbols with thick edges.

### 3. Implementation

Our implementation uses the MuMax3 finite-difference micromagnetics package [2], which is an open source code with a large user base (<https://mumax.github.io>). The implementation involves two steps, as discussed below.

#### 3.1. Eigenmode calculation

The first step involves calculating the eigenmode basis functions that are subsequently used for the mode filtering. We consider here the example of a magnetic vortex ground state in a 5- $\mu\text{m}$  diameter permalloy disk, which has been studied extensively by members of the NIMFEIA consortium [3–6]. The spin wave eigenmodes of this vortex state reflect the cylindrical symmetry of the system and are geometrically quantised with a radial mode number  $n$  and an azimuthal mode number  $m$ . The calculated dispersion relation for these spin wave eigenmodes for a 50-nm thick disk, shown for different  $n$  as a function of  $m$ , is presented in Figure 1.

The mode profiles and frequencies are obtained as follows. For a given  $(n, m)$ , we simulated the transient response of the magnetization to an excitation magnetic field of the form  $\mathbf{B}(\mathbf{r}, t) = (0, 0, b_{nm}(\mathbf{r})\text{sinc}(\omega_c t))$ , where the field amplitude  $b_{nm}(\mathbf{r})$  is taken to be



$$b_{nm}(\mathbf{r}) = b_0 J_1(\kappa_n \rho) e^{im\phi},$$

with  $b_0$  being a field amplitude,  $J_1$  the Bessel function of the first kind,  $\kappa_n$  a wave number that ensures mode quantisation along the radial direction  $\rho$ , and  $\phi$  the azimuthal direction in radial coordinates.  $\omega_c$  in the sinc function is the cut-off frequency and is taken to be 50 GHz. From the discrete Fourier transform of the transient response, we can identify the mode frequencies and profiles for each  $(n, m)$ . The spatial profile of each eigenmode,  $\psi_{nm}(\mathbf{r})$ , such as those shown in the right panel of Figure 1, is stored as an OOMMF format file (.ovf) for future use.

### 3.2. MuMax3 module for eigenmode projection

The second step involves projecting the magnetization dynamics onto the eigenmode profiles found above. To this end, we developed a module for the MuMax3 code, `ext_eigenmodeprojection.go`, which provides the following functionalities:

1. User-supplied transverse magnetization directions,  $\delta m_x(\mathbf{r})$  and  $\delta m_y(\mathbf{r})$ , implemented as `delta_mx` and `delta_my`, which are orthogonal to the micromagnetic ground state,  $\mathbf{m}_0(\mathbf{r})$ , i.e.,  $\mathbf{m}_0(\mathbf{r}) \cdot \delta m_{x,y}(\mathbf{r}) = 0$ . These profiles can be imported by calling

```
delta_mx.Add("filename.ovf", 1)
```

2. User-supplied eigenmode profile,  $\psi_{nm}(\mathbf{r})$ , such as those shown in the right panel of Figure 1, which is implemented as `psi_k`. This profile can be imported by calling

```
psi_k.Add("filename.ovf", 1)
```

3. Computed mode amplitude `a_k`, which returns the vector  $(a_{kx}, a_{ky}, \theta)$  where

$$a_{k,(x,y)}(t) = \int \psi_k(\mathbf{r}) \mathbf{m}(\mathbf{r}, t) \cdot \delta m_{x,y}(\mathbf{r}) dV.$$

```
TableAdd(a_k)
```

This module is available at the following fork of the MuMax3 repository:

<https://github.com/joovon/3/tree/master/engine>.

## 4. Results

An example of the application of this module to three-magnon scattering in the vortex system is shown in Figure 2. Following the study in Körber *et al.* [6], we follow the evolution of the directly-excited and scattered modes for an excitation frequency  $f_{\text{rf}}$  of 7.4 GHz and rf field amplitude of 3.5 mT at a temperature of 300 K. In Fig. 2(a), we can observe that the field excitation at this frequency directly populates the first-order radial mode  $(n = 1, m = 0)$ , which subsequently scatters into two  $m \neq 0$  modes with frequencies close to  $f_{\text{rf}}/2$ , indicated by the dashed red line, through the three-magnon splitting process.

In Fig. 2(b), we present selected mode powers computed using `ext_eigenmodeprojection.go`. For the directly-excited mode  $(n = 1, m = 0)$ , the mode power is observed to increase exponentially from its thermal value over an interval of less than 10 ns after application of the



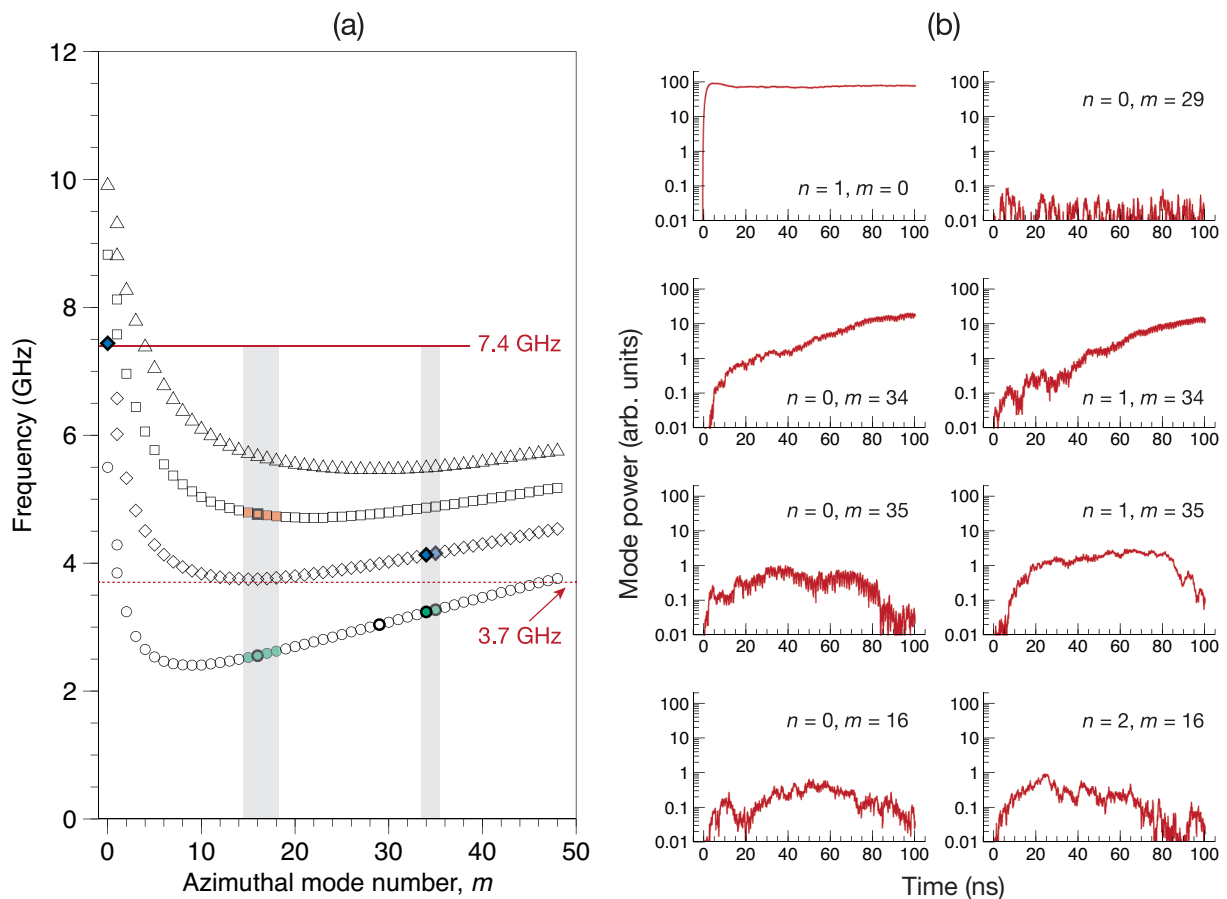


**Figure 2.** Three-magnon scattering with a excitation field at 7.4 GHz and amplitude of 3.5 mT. (a) Dispersion relation showing the rf excitation frequency  $f_{\text{rf}}$ , along with  $f_{\text{rf}}/2$  about which the scattered modes appear. Scattering mainly occurs in the gray zones, where mode frequencies are roughly equidistant from  $f_{\text{rf}}/2$ . Coloured dots indicate modes with powers about thermal values. (b) Selected mode powers for coloured symbols shown in (a). The power for  $(n = 0, m = 29)$  is representative of pure thermally-driven modes and provides a baseline for comparison with driven modes.

rf excitation, before saturating at a steady state value for the remainder of the simulation (total duration of 100 ns). As a point of comparison, the mode  $(n = 0, m = 29)$  is neither affected by the rf field excitation, nor by nonlinear scattering processes, and one can observe that its power remains at thermal values for the entire duration of the simulation. The largest power in the scattered modes is found for  $(n = 0, m = 34)$  and  $(n = 1, m = 34)$ , where a similar exponential growth is seen over the first 10 ns, followed by a slower linear growth with time after saturation of the directly-excited mode. These modes exhibit the strongest three-magnon scattering as their frequencies are roughly equidistant from  $f_{\text{rf}}/2$  and satisfy energy and angular-momentum conservation. Excitation above thermal levels can also be seen for the neighbouring  $(n = 0, 1; m = 35)$  modes, albeit with an order of magnitude less power and with a roll-off toward the end of the simulation. A similar behaviour can also be seen for the modes  $(n = 0, 2; m = 15 - 18)$  at lower azimuthal mode numbers, which are also roughly equidistant from  $f_{\text{rf}}/2$  but are excited to a lesser degree; an example for  $(n = 0; m = 16)$  and  $(n = 2; m = 16)$  is shown at the bottom of Fig. 2(b).



These results illustrate how the mode projection method can provide additional insight into the transient dynamics related to three-magnon scattering processes, which can be hard to access through frequency-domain analyses alone.

## 5. References

1. C. Abert, *Micromagnetics and Spintronics: Models and Numerical Methods*, The European Physical Journal B **92**, 33 (2019).
2. A. Vansteenkiste, J. Leliaert, M. Dvornik, M. Helsen, F. García-Sánchez, and B. V. Waeyenberge, *The Design and Verification of MuMax3*, AIP Advances **4**, 107133 (2014).
3. K. Schultheiss, R. Verba, F. Wehrmann, K. Wagner, L. Körber, T. Hula, T. Hache, A. Kakay, A. A. Awad, V. Tiberkevich, A. N. Slavin, J. Fassbender, and H. Schultheiss, *Excitation of Whispering Gallery Magnons in a Magnetic Vortex*, Physical Review Letters **122**, 097202 (2019).
4. L. Körber, K. Schultheiss, T. Hula, R. Verba, J. Fassbender, A. Kákay, and H. Schultheiss, *Nonlocal Stimulation of Three-Magnon Splitting in a Magnetic Vortex*, Physical Review Letters **125**, 207203 (2020).
5. R. Verba, L. Körber, K. Schultheiss, H. Schultheiss, V. Tiberkevich, and A. Slavin, *Theory of Three-Magnon Interaction in a Vortex-State Magnetic Nanodot*, Physical Review B **103**, 014413 (2021).
6. L. Körber, C. Heins, T. Hula, J.-V. Kim, H. Schultheiss, J. Fassbender, and K. Schultheiss, *Pattern recognition with a magnon-scattering reservoir*, arXiv:2211.02328.

